INTERNATIONAL JOURNAL FOR NUMERICAL METHODS IN FLUIDS, VOL. 9, 1183–1193 (1989)

NUMERICAL SOLUTION OF TRANSONIC FLOWS ON A STREAMFUNCTION CO-ORDINATE SYSTEM

RONALD M. BARRON AND R. K. NAEEM

Department of Mathematics and Statistics and Fluid Dynamics Research Institute (FDRI), University of Windsor, Windsor, Ontario, Canada N9B 3P4

SUMMARY

A new method has been developed for the computation of steady two-dimensional full-potential transonic flow past symmetric aerofoils. This method utilizes von Mises variables (x, ψ), where ψ is taken as the streamfunction for the flow. The flow equations and appropriate boundary conditions are formulated in terms of the von Mises variables (x, ψ) for symmetric aerofoils at zero incidence. This yields a system of two equations for unknowns $\rho(x, \psi)$ and $y(x, \psi)$. Finite difference solutions have been computed using SLOR at subcritical and supercritical Mach numbers. The results are compared with available data and are in excellent agreement.

KEY WORDS CFD Transonics Streamfunction co-ordinates

1. INTRODUCTION

Martin,[1] in a study of incompressible viscous fluids, introduced a natural curvilinear co-ordinate system (ϕ, ψ) in the physical plane (x, y) to investigate the geometry of flows. This 'streamline' method, ψ being the streamfunction, was first used by Grossman and Barron[2] to study incompressible inviscid flows numerically. They found that it was not possible to determine analytically where the leading and trailing edges are mapped into the (ϕ, ψ) system and that numerically obtained values for the leading and trailing edges are not very accurate, resulting in inaccuracies in the solution near these points. During a study of inviscid incompressible flows, Barron[3] found that by introducing von Mises variables (x, ψ), one knows exactly where the leading and trailing edges are mapped in the (x, ψ) plane and inaccuracies in the solution near the leading and trailing edges can be eliminated.

In Barron's approach the co-ordinate ψ is taken as the streamfunction for the flow being considered. This approach provides a rectangular computational domain, circumventing the need to do grid generation. Furthermore, a Dirichlet formulation of the problem is possible. In the present paper we have extended Barron's approach to the case of inviscid compressible fluids. The flow equations are transformed into von Mises variables and are solved subject to appropriate boundary conditions for a class of transonic flows over symmetric aerofoils. The class that has been considered is that for which the flow is isentropic and irrotational. Subcritical and supercritical cases have been considered and computed results are in excellent agreement with available results.

0271–2091/89/101183–11$05.50

Received 15 February 1988
Revised 17 October 1988

2. FLOW EQUATIONS

The steady two-dimensional adiabatic flow of an inviscid compressible fluid is governed by the following system of equations:

$$(\rho u)_x + (\rho v)_y = 0 \qquad \text{(continuity)}, \tag{1}$$

$$\left.\begin{aligned} \rho(uu_x + vu_y) + p_x &= 0 \\ \rho(uv_x + vv_y) + p_y &= 0 \end{aligned}\right\} \qquad \text{(Navier–Stokes)}, \tag{2}$$

$$uS_x + vS_y = 0 \qquad \text{(energy)}, \tag{3}$$

$$\rho = \rho(p, S) \qquad \text{(state equation)}. \tag{4}$$

This is a system of four equations wherein ρ is the density, p the pressure, S the specific entropy, and u and v are the velocity components in the x and y directions. For convenience in the following analysis, the dependent variables are non-dimensionalized by free stream quantities ρ_∞, V_∞, p_∞ and S_∞, while the independent variables are non-dimensionalized by the characteristic length L.

On introducing the vorticity function ω defined by

$$\omega = v_x - u_y, \tag{5}$$

equation (2) is replaced by

$$\left.\begin{aligned} \left[\frac{V^2}{2} + \frac{p}{\rho}\right]_x - v\omega + \frac{p\rho_x}{\rho^2} &= 0, \\ \left[\frac{V^2}{2} + \frac{p}{\rho}\right]_y + u\omega + \frac{p\rho_y}{\rho^2} &= 0, \end{aligned}\right\} \tag{6}$$

where $V^2 = u^2 + v^2$.

Following Martin,[1] we introduce curvilinear co-ordinates ϕ, ψ in which the curves $\psi =$ constant are later taken as the streamlines and the curves $\phi =$ constant are left arbitrary so that the physical co-ordinates x, y can be replaced by ϕ, ψ.

Let

$$\mathbf{r} = (x, y) = \mathbf{r}(\phi, \psi) \tag{7}$$

define a system of curvilinear co-ordinates in the (x, y) plane such that the Jacobian J defined by

$$J = |\mathbf{r}_\phi \times \mathbf{r}_\psi|$$

is non-zero in the region of interest.

The squared element of arc length can be represented by

$$\begin{aligned} \mathrm{d}s^2 &= \mathrm{d}\mathbf{r} \cdot \mathrm{d}\mathbf{r} \\ &= E(\phi, \psi)\mathrm{d}\phi^2 + 2F(\phi, \psi)\mathrm{d}\phi\mathrm{d}\psi + G(\phi, \psi)\mathrm{d}\psi^2, \end{aligned} \tag{8}$$

where the metrics are given by

$$\begin{aligned} E(\phi, \psi) &= \mathbf{r}_\phi \cdot \mathbf{r}_\phi, \\ F(\phi, \psi) &= \mathbf{r}_\phi \cdot \mathbf{r}_\psi, \\ G(\phi, \psi) &= \mathbf{r}_\psi \cdot \mathbf{r}_\psi. \end{aligned} \tag{9}$$

The partial derivatives in the (x, y) and (ϕ, ψ) systems are related by

$$\begin{aligned} \mathbf{r}_\phi &= J(\psi_y, -\psi_x), \\ \mathbf{r}_\psi &= J(-\phi_y, \phi_x). \end{aligned} \tag{10}$$

Let $\alpha(\phi, \psi)$ be the angle between the tangent vector (x_ϕ, y_ϕ) to the co-ordinate line $\psi = \text{constant}$ and the x-axis; then[1]

$$\mathbf{r}_\phi = \sqrt{E}\,(\cos\alpha, \sin\alpha),$$

$$\mathbf{r}_\psi = \frac{F}{\sqrt{E}}(\cos\alpha, \sin\alpha) - \frac{J}{\sqrt{E}}(\sin\alpha, -\cos\alpha),$$

$$\alpha_\phi = \frac{J}{E}\Gamma^2_{11},$$

$$\alpha_\psi = \frac{J}{E}\Gamma^2_{12},$$

where Γ^2_{11} and Γ^2_{12} are Christoffel symbols given by

$$\Gamma^2_{11} = \frac{1}{2J^2}[-FE_\phi + 2EF_\phi - EE_\psi],$$

$$\Gamma^2_{12} = \frac{1}{2J^2}[EG_\phi - FE_\psi].$$

The integrability condition on α, i.e. $\alpha_{\phi\psi} = \alpha_{\psi\phi}$, leads to the Gauss equation

$$K = \frac{1}{W}\left[\left(\frac{W}{E}\Gamma^2_{11}\right)_\psi - \left(\frac{W}{E}\Gamma^2_{12}\right)_\phi\right] = 0, \tag{11}$$

where $W = \sqrt{(EG - F^2)}$ and K is called the Gaussian curvature. This equation represents a necessary and sufficient condition that E, F and G are the coefficients of the first fundamental form (8).

We now proceed to write equations (1) and (3)–(6) in the (ϕ, ψ) curvilinear co-ordinates, where ψ is defined as the streamfunction. Equation (1) implies the existence of the streamfunction $\psi(x, y)$ such that

$$\rho u = \psi_y, \qquad \rho v = -\psi_x. \tag{12}$$

Chandna *et al.*[4] have shown that the equation of continuity (1) is equivalent to

$$E = \rho^2 J^2 V^2, \tag{13}$$

where

$$J^2 = EG - F^2. \tag{14}$$

The momentum equations (6) become

$$\left[\frac{V^2}{2} + \frac{p}{\rho}\right]_\phi + \frac{p\rho_\phi}{\rho^2} = 0,$$

$$\left[\frac{V^2}{2} + \frac{p}{\rho}\right]_\psi + \frac{\omega}{\rho} + \frac{p\rho_\psi}{\rho^2} = 0. \tag{15}$$

In Reference 4 it has also been shown that the vorticity function (5) in the (ϕ, ψ) system is given by

$$\omega = \frac{1}{W}\left[\left(\frac{F}{\rho W}\right)_\phi - \left(\frac{E}{\rho W}\right)_\psi\right]. \tag{16}$$

Employing equations (10) and (2) in (3), we obtain, after some manipulation,

$$S_\phi = 0. \tag{17}$$

Hence, in the (ϕ, ψ) system, the flow is governed by equations (4), (13), (15)–(17) and the Gauss equation (11). These are seven equations for the eight unknowns E, F, G, V, ρ, p, ω and S. This system is undetermined as a result of the arbitrariness in the function ϕ.

3. VON MISES TRANSFORMATION

Barron[3] indicated that for irrotational flows the arbitrariness of ϕ causes difficulties, particularly in the location of the leading and trailing edges and in the application of the flow tangency condition on the surface of the body. To overcome these difficulties, he introduced von Mises variables (x, ψ) through the transformation

$$x = \phi, \qquad y = y(\phi, \psi). \tag{18}$$

On introducing these von Mises variables (x, ψ), equations (4), (13) and (15)–(17) are replaced by the following equations:

$$\sqrt{E} = \rho V W, \tag{19}$$

$$\left[\frac{V^2}{2} + \frac{p}{\rho}\right]_x + \frac{p\rho_x}{\rho^2} = 0, \tag{20}$$

$$\left[\frac{V^2}{2} + \frac{p}{\rho}\right]_\psi + \frac{\omega}{\rho} + \frac{p\rho_\psi}{\rho^2} = 0, \tag{21}$$

$$\omega = \frac{1}{W}\left[\left(\frac{F}{\rho W}\right)_x - \left(\frac{E}{\rho W}\right)_\psi\right], \tag{22}$$

$$S_x = 0, \tag{23}$$

$$\rho = \rho(p, S) \tag{24}$$

where

$$E = 1 + y_x^2, \qquad F = y_x y_\psi, \qquad W = y_\psi.$$

Here we have assumed that $J = W > 0$, which is equivalent to requiring that the fluid flows from lower to higher values of ϕ,[1] i.e. in the direction of the positive x-axis.

Let

$$y = f(x) \tag{25}$$

be the equation of the upper surface of a symmetric aerofoil and assume that flow is uniform in the far field, parallel to the chord of the aerofoil. In the physical plane the appropriate boundary conditions are

(i) far-field conditions:

$$\left.\begin{aligned} \rho &= 1 \\ u &= 1 \\ v &= 0 \end{aligned}\right\} \quad \text{as } x^2 + y^2 \to \infty, \tag{26}$$

(ii) tangency conditions and flow symmetry:

$$v/u = \begin{cases} f'(x) & \text{on } y = f(x), \quad x_{LE} \leqslant x \leqslant x_{TE}, \\ 0 & \text{on } y = 0, \quad x < x_{LE} \quad \text{or} \quad x > x_{TE}, \end{cases} \tag{27}$$

where the prime represents the derivative with respect to x, and x_{LE} and x_{TE} denote the leading and trailing edges respectively.

These conditions are conveniently expressed in the (x, ψ) plane by referring to the aerofoil surface as a segment of the streamline $\psi = 0$. We have

(i) far-field conditions:

$$\left.\begin{aligned} \rho &= 1 \\ y &= \psi \end{aligned}\right\} \quad \text{at } \infty, \tag{28}$$

(ii) tangency condition and flow symmetry:

$$y = \begin{cases} f(x) & \text{on } \psi = 0, \quad x_{LE} \leqslant x \leqslant x_{TE}, \\ 0 & \text{on } \psi = 0, \quad -\infty < x < x_{LE} \quad \text{or} \quad x_{TE} < x < \infty. \end{cases} \tag{29}$$

As mentioned in the introduction, we are interested in that class of transonic flows which are irrotational and isentropic. Therefore the state equation in non-dimensional form is

$$p = \rho^{\gamma}/\gamma M_{\infty}^2, \qquad M_{\infty} = V_{\infty}/a_{\infty}, \tag{30}$$

where $\gamma (= 1{\cdot}4$ for air) is the adiabatic constant, and M_{∞} and a_{∞} are the free stream Mach number and speed of sound respectively.

Employing (19) and (30) in (20), (21) and integrating (with $\omega = 0$), we get

$$\frac{1 + y_x^2}{\rho^2 y_{\psi}^2} + \frac{2\rho^{\gamma - 1}}{(\gamma - 1)M_{\infty}^2} = 1 + \frac{2}{(\gamma - 1)M_{\infty}^2}, \tag{31}$$

which is Bernoulli's equation.

Taking $\omega = 0$, using the expressions for E, F and W in terms of y_x and y_{ψ}, and expanding (22) yields

$$y_{\psi}^2 y_{xx} - 2y_x y_{\psi} y_{\psi x} + (1 + y_x^2) y_{\psi\psi} = \frac{y_{\psi}^2 y_x \rho_x}{\rho} - \frac{y_{\psi}(1 + y_x^2)\rho_{\psi}}{\rho}. \tag{32}$$

It should be noted that the above equation is the extension of the incompressible potential flow equation to compressible full-potential flow. For constant density the right-hand side of (32) is zero.[3]

Summarizing, the well posed boundary value problem for full-potential transonic flow over symmetric aerofoils is to solve equations (31) and (32) subject to boundary conditions (28) and (29).

One can easily show that the pressure coefficient is given by

$$C_p = 2(\rho^{\gamma} - 1)/\gamma M_{\infty}^2. \tag{33}$$

The Bernoulli equation (31) can be rewritten as

$$\rho = \left[1 - \frac{(\gamma - 1)M_{\infty}^2}{2}\left(\frac{1 + y_x^2}{\rho^2 y_{\psi}^2} - 1\right)\right]^{1/(\gamma - 1)}. \tag{34}$$

This equation implies that there are two values of the density for a certain mass flux less than the maximum value which can be attained.[5] For purely subsonic or supersonic flows one can easily decide which value to choose depending upon whether ρ is larger or smaller than ρ^*, the value of the density at the critical speed of sound a^*, respectively. For mixed flows it is not obvious which value to choose. To overcome this problem, researchers have developed artificial viscosity[6] and artificial compressibility[7,8] methods. In both methods the density is modified by introducing an artificial viscosity term which vanishes in subsonic regions. Details can be obtained from Reference 6.

In our calculations we employ an expression for the modified density which is similar to that proposed by Hafez *et al*[7]. The modified density $\tilde{\rho}$ is given by

$$\tilde{\rho} = \rho - (\mu \rho_x \Delta x). \tag{35}$$

Here μ is the switching function, which vanishes in the subsonic region, defined by

$$\mu = \max(0, 1 - 1/M^2), \tag{36}$$

where M is the local Mach number.

4. DISCRETIZATION OF EQUATIONS

Equation (32) is discretized by using central differencing for all derivatives everywhere. This leads to a large system of non-linear algebraic equations in unknown y at the grid points. The finite difference approximation of equation (32) at an (i,j) grid point is

$$\begin{aligned} &A_1(y_{i+1,j} - 2y_{ij} + y_{i-1,j}) + A_2(y_{i+1,j+1} + y_{i-1,j-1} - y_{i-1,j+1} - y_{i+1,j-1}) \\ &+ A_3(y_{i,j+1} - 2y_{ij} + y_{i,j-1}) = A_4 \frac{\tilde{\rho}_{i+1,j} - \tilde{\rho}_{i-1,j}}{\tilde{\rho}_{ij}} + A_5 \frac{\tilde{\rho}_{i,j+1} - \tilde{\rho}_{i,j-1}}{\tilde{\rho}_{ij}}, \end{aligned} \tag{37}$$

where

$$A_1 = \left(\frac{y_{i,j+1} - y_{i,j-1}}{2\Delta\psi} \right)^2,$$

$$A_2 = \frac{-(y_{i,j+1} - y_{i,j-1})(y_{i+1,j} - y_{i-1,j})}{8(\Delta\psi)^2},$$

$$A_3 = \beta^{*2} \left[1 + \left(\frac{y_{i+1,j} - y_{i-1,j}}{2\Delta\psi} \right)^2 \right],$$

$$A_4 = \frac{\beta^*}{8} \frac{(y_{i+1,j} - y_{i-1,j})(y_{i,j+1} - y_{i,j-1})^2}{\Delta\psi},$$

$$A_5 = -\frac{\beta^{*2}}{4} (y_{i,j+1} - y_{i,j-1}) \left[1 + \left(\frac{y_{i+1,j} - y_{i-1,j}}{2\Delta x} \right)^2 \right],$$

$$\tilde{\rho}_{ij} = \rho_{ij} - \mu_{ij} (\rho_x \Delta x)_{ij},$$

$$\rho_{ij} = \left(1 + \frac{(\gamma - 1) M_\infty^2}{2} - \frac{(\gamma - 1) M_\infty^2}{2} A_6 \right)^{1/(\gamma - 1)},$$

$$A_6 = 4\Delta\psi^2 \left[1 + \left(\frac{y_{i+1,j} - y_{i-1,j}}{2\Delta x} \right)^2 \right] \Big/ \tilde{\rho}_{ij}^2 (y_{i,j+1} - y_{i,j-1})^2,$$

$$\mu_{ij} = \max(0, 1 - 1/M_{ij}^2), \qquad \beta^* = \Delta x / \Delta\psi.$$

Equation (37) in matrix form can be written as

$$\mathbf{N}\mathbf{y} = \mathbf{R}, \tag{38}$$

where the matrix $\mathbf{N}$ contains the coefficients A_1, A_2 and A_3, the elements of $\mathbf{y}$ consist of the function y for each point in the computational domain, and the vector $\mathbf{R}$ contains specified boundary values and the right-hand side of (37).

In the entire flow region ρ and $\tilde{\rho}$ are computed using central differencing for derivatives y_x and y_ψ except along the line $\psi = 0$. Along $\psi = 0$ (i.e. $j = 1$), y_ψ and y_x are computed from

$$y_\psi|_{i1} = \frac{y_{i2} - y_{i1}}{\Delta\psi},$$

$$y_x|_{i1} = \begin{cases} f'(x_i), & x_{LE} \leqslant x_i \leqslant x_{TE}, \\ 0 & -\infty < x_i < x_{LE} \text{ or } x_{TE} < x_i < \infty. \end{cases}$$

For speed calculations, differencing for derivatives y_ψ and y_x is the same as above except in the supersonic region, where y_x is computed from

$$y_x|_{ij} = \frac{y_{ij} - y_{i-2,j}}{2\Delta x}.$$

The matrix equation (38) was solved using SLOR. In order to improve the accuracy, to reduce CPU time and to pack grid lines near the aerofoil and at the leading and trailing edges, we introduce stretching transformations in the next section.

5. STRETCHING TRANSFORMATIONS

Following Jones,[9] we introduce transformations defined by

$$x = A \tan\xi \exp(-B\xi^2),$$
$$\psi = D \tan\eta. \tag{39}$$

These transformations transfer $x = \pm\infty$ and $\psi = \pm\infty$ to $\xi = \pm\pi/2$ and $\eta = \pm\pi/2$ respectively. Another benefit of these transformations is that they provide us with a dense mesh in the vicinity of the aerofoil. The former helps to make mesh points more dense near leading and trailing edges of the aerofoil and the latter packs more points near the x-axis.

For convenience in handling the boundary conditions at infinity, we introduce a new variable Y defined by

$$y = Y + \psi. \tag{40}$$

Employing (39) and (40) in (32), we get

$$B_1 Y_{\xi\xi} + B_2 Y_{\eta\eta} + B_3 Y_{\eta\xi} + B_4 Y_\xi + B_5 Y_\eta = \psi_\eta^2 x_\xi^2 B_6, \tag{41}$$

where

$$B_1 = [\psi_\eta + Y_\eta]^2, \qquad B_2 = [x_\xi^2 + Y_\xi^2], \qquad B_3 = -2Y_\xi[Y_\eta + \psi_\eta],$$

$$B_4 = -[\psi_\eta + Y_\eta]^2 \frac{x_{\xi\xi}}{x_\xi}, \quad B_5 = -[x_\xi^2 + Y_\xi^2]\frac{\psi_{\eta\eta}}{\psi_\eta},$$

$$B_6 = \frac{Y_\xi[\psi_\eta + Y_\eta]^2\tilde{\rho}_\xi}{\tilde{\rho}} - \frac{[\psi_\eta + Y_\eta][x_\xi^2 + Y_\xi^2]\tilde{\rho}_\eta}{\tilde{\rho}}$$

and $\tilde{\rho}$ is defined in Section 4.

The boundary conditions in the (ξ, η) system are

$$Y = \begin{cases} f(\xi) & \text{on } \eta = 0, \quad \xi_{LE} \leqslant \xi \leqslant \xi_{TE}, \\ 0 & \text{on } \eta = 0, \quad -\pi/2 < \xi < \xi_{LE} \quad \text{or} \quad \xi_{TE} < \xi < \pi/2, \end{cases}$$

$$\left.\begin{matrix} Y = 0 \\ \tilde{\rho} = \rho = 1 \end{matrix}\right\} \quad \xi = \pm\pi/2 \quad \text{or} \quad \eta = \pi/2.$$

Here ξ_{LE} and ξ_{TE} are the values of x_{LE} and x_{TE} respectively in the (ξ, η) plane.

The discretization of equations in the stretched co-ordinates and the corresponding numerical algorithm are the same as in Section 4.

6. RESULTS AND DISCUSSION

During the investigation it was found that if the term ρ_x in (35) is calculated from (31), the results obtained are more satisfactory. Throughout the calculations ρ and $\tilde{\rho}$ are relaxed through the relations

$$\rho_{ij}^{(n+1)} = (1-\omega_1)\rho_{ij}^{(n)} + \omega_1 \, [\text{equation (34)}]^{(n)},$$

$$\tilde{\rho}_{ij}^{(n+1)} = (1-\omega_2)\tilde{\rho}_{ij}^{(n)} + \omega_2[\rho_{ij}^{(n)} - \mu_{ij}^{(n)}\rho_{xij}^{(n)}\Delta x],$$

where n is the nth iteration level, and ω_1 and ω_2 are relaxation parameters. After some experimentation it was found that the values 0·7 and 0·5 for relaxation parameters ω_1 and ω_2 respectively give the most satisfactory results. For our purpose the constants A, B and D in transformation (39) are kept constant at 0·9, 0·6 and 0·4 respectively. Jones[9] has discussed in detail how the constants in transformation (39) are chosen.

The NACA 0012-64 and 6% circular arc aerofoils were tested with this new formulation. The results have been computed for these aerofoils at subcritical and supercritical Mach numbers. Uniform and stretched grids were employed. Comparisons with the results obtained by other researchers have been made in Figures 1–4. For subcritical flows (Figures 1, 2 and 4) excellent

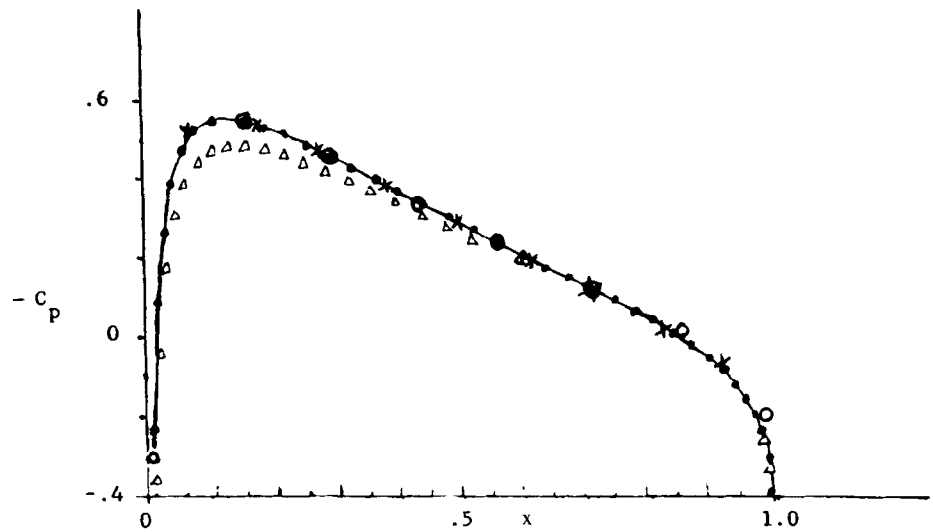

Figure 1. Surface pressure distribution, NACA 0012, $M_\infty = 0{\cdot}63$: △, panel method;[10] ●, Sinclair;[10] ——, Garabedian–Korn;[11] ○, present (non-stretched co-ordinates); ×, present (stretched co-ordinates)

agreement is obtained on both the clustered and non-clustered grids. However, the same accuracy is achieved for the packed grid using about half as many grid points in each direction as compared to the non-clustered solution. Furthermore, the CPU time is reduced by a factor of about 1/5. The clustered grid solution provides slightly more accuracy for the supercritical flow at $M_\infty = 0{\cdot}8$ over

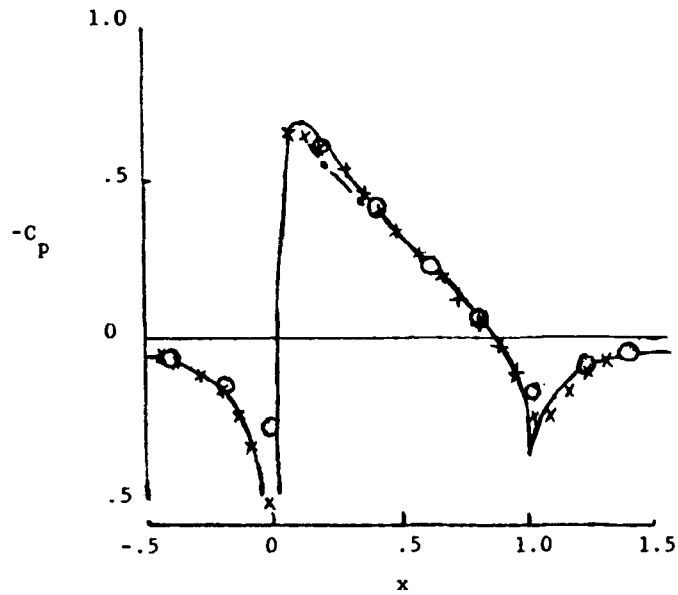

Figure 2. Surface pressure distribution, NACA 0012, $M_\infty = 0{\cdot}7$: —.—, irrotational;[8] ——, Hafez–Lovell;[8] ○, present (non-stretched co-ordinates); ×, present (stretched co-ordinates)

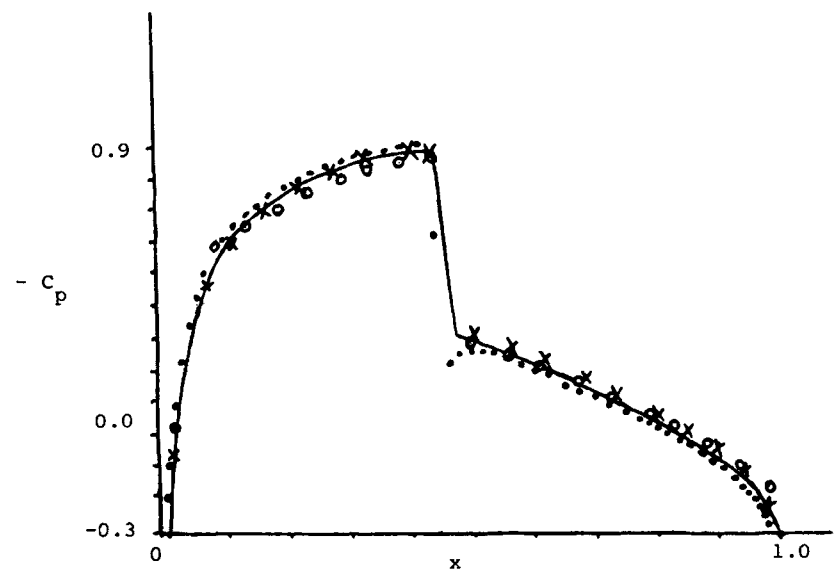

Figure 3. Surface pressure distribution, NACA 0012, $M_\infty = 0{\cdot}8$: ●, Sinclair;[10] ——, Garabedian–Korn;[11] ○, present (non-stretched grid); ×, present (stretched grid)

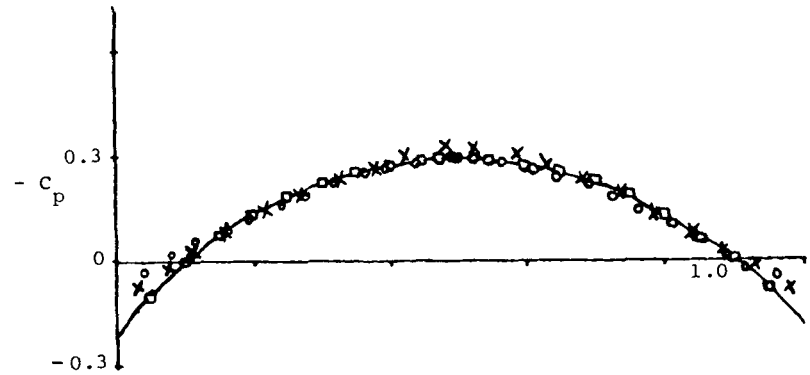

Figure 4. Surface pressure distribution, 6% circular arc aerofoil, $M_\infty = 0{\cdot}817$: ⊟⊟, Earl;[12] ○, present (non-stretched grid); ×, present (stretched grid)

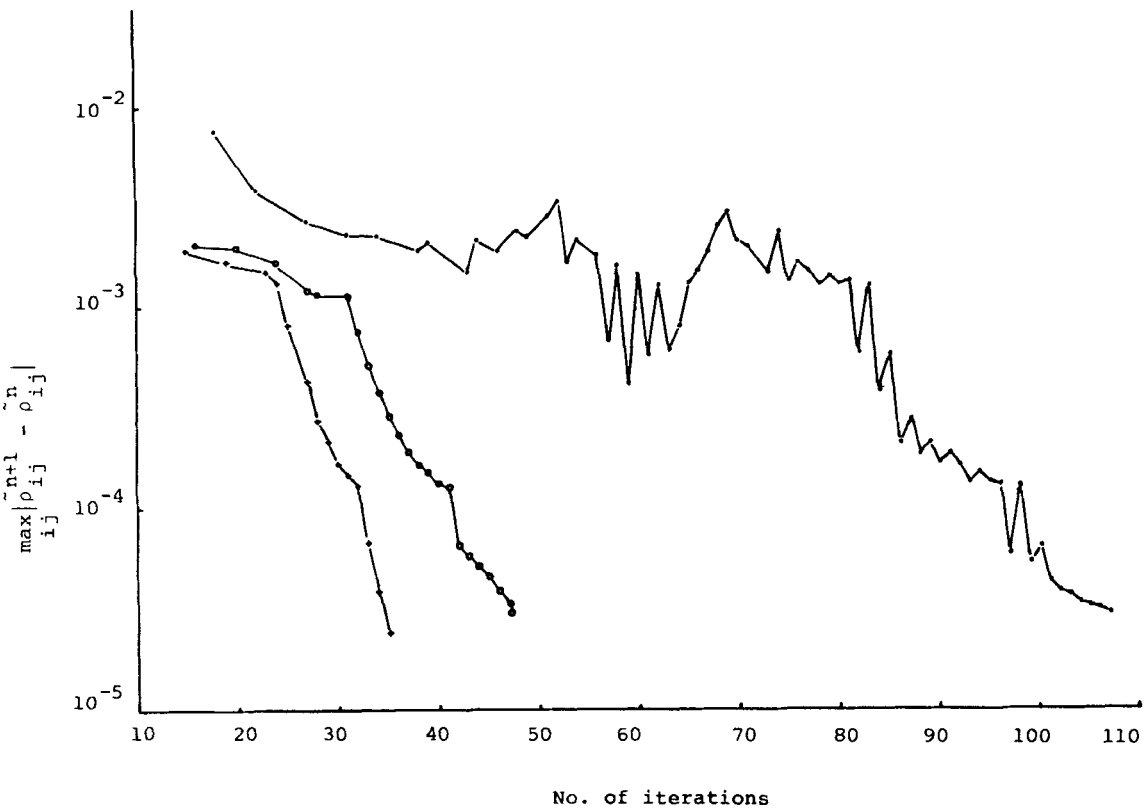

Figure 5. Convergence histories for $\tilde{\rho}$, NACA 0012: +, $M_\infty = 0{\cdot}63$; ○, $M_\infty = 0{\cdot}7$; ●, $M_\infty = 0{\cdot}8$

the NACA 0012 aerofoil, particularly aft of the shock wave. Both solutions compare favourably with the results of Sinclair[10] and Garabedian and Korn.[11]

The convergence history for the density is shown in Figure 5 for the NACA 0012. At subcritical free stream Mach numbers of 0·63 and 0·7 the convergence is very fast and well behaved. For the

supercritical flow at $M_\infty = 0{\cdot}8$ the error oscillates before damping out at approximately 100 iterations. Runs were made at various grid sizes for all cases and the results presented correspond to clustered grids of 25×18, 35×15 and 49×16 for $M_\infty = 0{\cdot}63$, $0{\cdot}7$ and $0{\cdot}8$ respectively.

7. CONCLUSIONS

Inviscid compressible potential equations have been transformed into von Mises variables (x, ψ), leading to a non-linear partial differential equation for the unknown $y(x, \psi)$ and an algebraic equation for the density. The transonic flow over a symmetric aerofoil is formulated as a Dirichlet boundary value problem and solved using finite differences. The supersonic region which occurs in supercritical flow is handled using the modified density method. Results are in excellent agreement with previous results. The numerical algorithm is efficient and easy to code.

ACKNOWLEDGEMENT

This research has been supported by a grant from the Natural Sciences and Engineering Research Council of Canada.

REFERENCES

1. M. H. Martin, 'The flow of a viscous fluid I', *Arch. Rat. Mech. Anal.* **41,** 266–286 (1971).
2. G. W. Grossman and R. M. Barron, 'A new approach to the solution of Navier–Stokes equations', *Int. j. numer. methods fluids*, **17,** 1315–1324 (1987).
3. R. M. Barron, 'Computation of incompressible potential flow using von Mises co-ordinates', *Mathematics and Computers in Simulation*, in press, (1989).
4. O. P. Chandna, R. M. Barron and M. R. Garg, 'Plane compressible MHD flows', *Q. Appl. Math.*, **26,** 411–422 (1979).
5. J. L. Steger, 'Application of cyclic relaxation procedures to transonic flow fields', *Ph.D. Dissertation*, Iowa State University, 1969.
6. A. Jameson, 'Numerical computation of transonic flows with shock waves', *Symposium Transsonicum III*, Springer-Verlag, New York, 1976, pp. 384–414.
7. M. Hafez, E. M. Murman and J. South, 'Artificial compressibility methods for numerical solution of transonic full-potential equation', *AIAA Paper 78-1148*, 1978.
8. M. Hafez and D. Lovell, 'Numerical solution of transonic stream function equation', *AIAA J.*, **21,** 327–334 (1983).
9. D. J. Jones and R. G. Dickinson, 'A description of the NAE two-dimensional transonic small disturbance computer method', *NAE Laboratory Technical Report LTR-HA-39*, January 1980.
10. P. M. Sinclair, 'An exact integral (field panel) method for the calculation of two dimensional transonic potential flow around complex configurations', *Aeronaut. J.*, **90** (896), 227–236 (1986).
11. P. R. Garabedian and D. Korn, 'Analysis of transonic airfoils', *Comm. Pure Appl. Math.*, **24,** 841–851 (1971).
12. D. K. Earl, 'Experimental investigation at transonic speeds of pressure distributions over wedge and circular arc airfoil sections and evaluation of perforated wall interference', *NASA TN D-15*, March 1959.